

## Light Curve Analysis of the Hybrid SdB Pulsators HS 0702+6043 and HS 2201+2610

R. Lutz,<sup>1</sup> S. Schuh,<sup>1</sup> R. Silvotti,<sup>2</sup> S. Dreizler,<sup>1</sup> E. M. Green,<sup>3</sup>  
G. Fontaine,<sup>4</sup> T. Stahn,<sup>5</sup> S. D. Hügelmeyer,<sup>1</sup> and T.-O. Husser<sup>1</sup>

<sup>1</sup>*Institut für Astrophysik, Georg-August-Universität Göttingen,  
Friedrich-Hund-Platz 1, 37077 Göttingen, Germany*

<sup>2</sup>*INAF-Osservatorio Astronomico di Capodimonte, via Moiariello 16,  
80131 Napoli, Italy*

<sup>3</sup>*Steward Observatory, University of Arizona, 933 North Cherry Ave.,  
Tucson, AZ 85721, USA*

<sup>4</sup>*Département de Physique, Université de Montréal, C.P. 6128,  
Succursale Centre-Ville, Montréal, Québec, H3C 3J7, Canada*

<sup>5</sup>*Max-Planck-Institut für Sonnensystemforschung, Max-Planck-Straße 2,  
37191 Katlenburg-Lindau, Germany*

**Abstract.** We present the detection of low-amplitude, long-period  $g$ -modes in two individual sdBV stars which are known to be  $p$ -mode pulsators. Only few of these hybrid objects, showing both  $p$ - and  $g$ -modes, are known today. We resolve the  $g$ -mode domain in HS 0702+6043 and add HS 2201+2610 to the list of hybrid pulsators. To discover the low-amplitude  $g$ -modes, a filtering algorithm based on wavelet transformations was applied to denoise observational data.

### 1. Introduction

Subdwarf B stars are evolved and compact objects which are thought to be core helium burning. They populate the extreme horizontal branch (EHB) at effective temperatures of 20 000 – 40 000 K and surface gravities  $\log(g/\text{cm s}^{-2})$  between 5.0 and 6.2. Variable sdB stars (sdBVs) can be divided into the following subclasses: The  $p$ -mode pulsators show higher amplitudes and shorter periods at higher temperatures. Kilkenney et al. (1997) discovered EC 14026-2647 as the class prototype. The  $g$ -mode pulsators have lower amplitudes and longer periods at lower temperatures and the class prototype PG 1716+426 was discovered by Green et al. (2003). Hybrid pulsators show both  $p$ - and  $g$ -modes. These are particularly exciting objects, since the two mode types probe different regions in the star. Both mode types are thought to be driven by the same  $\kappa$ -mechanism (Charpinet et al. 1997; Fontaine et al. 2003; Jeffery & Saio 2006). Figure 1 shows the location of some sdB pulsators in the  $\log g - T_{\text{eff}}$  diagram.

### 2. Observations, Data Reduction and Wavelet Filter

The HS 0702+6043 photometric data have been taken at the Calar Alto Observatory in January 2005 with the 2.2 m telescope equipped with CAFOS, using a B filter. From the whole ten day data set we used the best six nights ( $\approx 56$  hours)

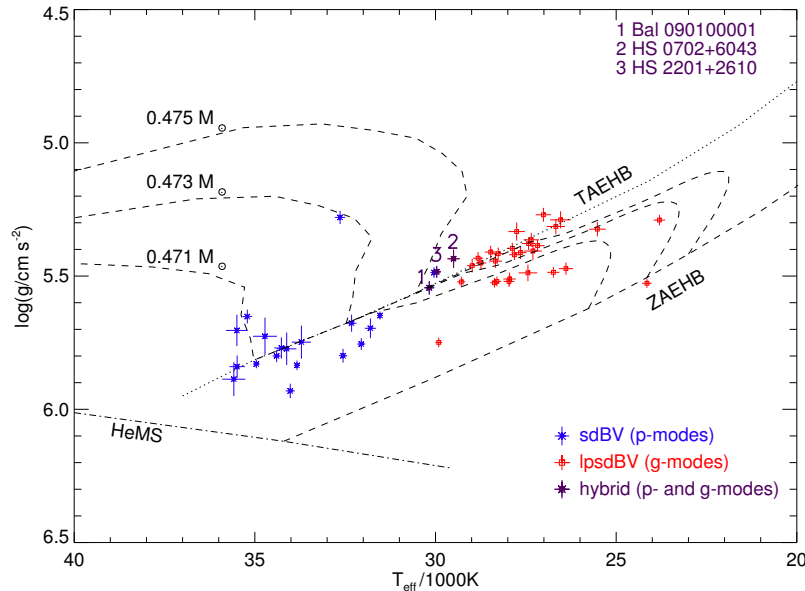


Figure 1. Location of some known sdB pulsators in the  $\log g$ - $T_{\text{eff}}$  diagram. Evolutionary tracks (Dorman, O’Connell, & Rood 1995) for three stellar masses are indicated, as well as helium main sequence (HeMS) and zero age (ZAEHB) and terminal age (TAEHB) extreme horizontal branches. The positions (taken from E. M. Green and G. Fontaine; for a discussion see also Green et al., these proceedings) clearly reveal two instability regions. The three known hybrid pulsators are labelled 1, 2 and 3.

for a further analysis after subtraction of the  $p$ -modes. The HS 2201+2610 data have also been taken at Calar Alto Observatory in September and November 2006 with the same setup as above. Five nights of observation yield a total of about 26 hours of high S/N photometric data. We reduced the data in a standard way, using the aperture photometry package TRIPP (Schuh et al. 2003). To denoise our HS 0702+6043 data, we applied the so-called *à trous* algorithm (Fligge & Solanki 1997) which is based on wavelet transformations. The basic procedure of the filter is to decompose the noisy light curve into different scales, i.e. different frequency bands, and to compare transformation coefficients to a simulated pure noise light curve. Setting a threshold value during the reconstruction therefore produces a filtered and denoised light curve.

### 3. Frequency Analysis of HS 0702+6043 and HS 2201+2610

The following frequency spectra (Lomb-Scargle-Periodograms, LSPs) have been generated using the Scargle algorithm, because it can handle unevenly sampled data. The confidence levels (derived from false alarm probabilities) are based on ten thousand white noise simulations. Figure 2 shows the window functions. The hybrid character of HS 0702+6043 is described in Schuh et al. (2006) and with the 2005 data presented here, we are able to provide a better resolution of the  $g$ -mode domain. The results of our frequency analysis are summarized in the

top part of Table 1. Figure 3 displays the  $g$ -mode regime. In our 2006 data of HS 2201+2610 we detect a long-period variation shown in Figure 4. Other data provided by one of us (R. S.) also show this variation. Our frequency analysis is summarized in the bottom part of Table 1. In addition to the hybrid behaviour, the interest for HS 2201+2610 increased a lot recently due to the presence of an orbiting planet (Silvotti et al. 2007, and these proceedings).

#### 4. Results

We resolve three gravity modes in the hybrid pulsator HS 0702+6043 and detect a long-period variation in HS 2201+2610. We therefore propose to add the latter to the list of hybrid pulsators.

Table 1. Frequencies appearing in HS 0702+6043 (top) and HS 2201+2610 (bottom). *Top*: We estimate the errors in the frequency to be  $0.9 \mu\text{Hz}$  (main FWHM in the window function) and having an accuracy of half a mmi in the amplitudes at a detection limit of 0.8 mmi. *Bottom*: We estimate the errors in the frequency to be  $0.5 \mu\text{Hz}$  and having a detection limit of 1.1 mmi. We used (f4) and (f5) in the prewhitening, because low-amplitude signals in this frequency range were also found in other runs (Silvotti et al. 2002).

Object	ID	Frequency [ $\mu\text{Hz}$ ]	Period [s]	Amplitude [mmi]	type
HS 0702+6043	f1	2753.9	363.1	21.7	$p$
	f2	2606.1	383.7	4.6	$p$
	f3	271.7	3680.8	1.8	$g$
	f4	318.1	3144.2	1.3	$g$
	f5	206.3	4847.0	0.9	$g$
HS 2201+2610	f1	2861.2	349.5	6.6	$p$
	f2	2823.7	354.2	3.3	$p$
	f3	2880.8	347.1	1.5	$p$
	(f4)	2725.9	366.9	0.8	$p$
	(f5)	2906.3	344.1	0.4	$p$
	f6	307.2	3255.6	1.5	$g$

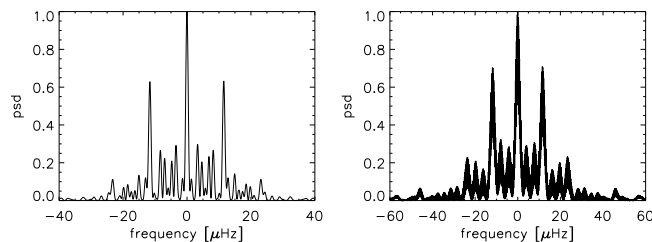


Figure 2. Window functions of our HS 0702+6043 (left) and HS 2201+2610 data (right).

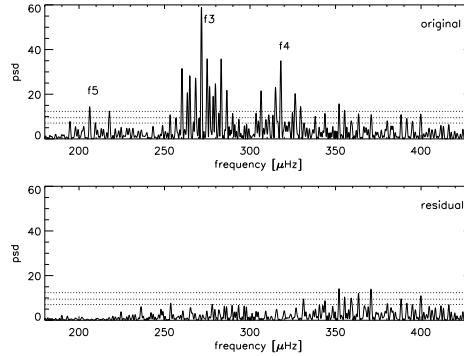


Figure 3. LSPs of the  $g$ -mode regime of HS 0702+6043 after subtraction of two  $p$ -modes (top). Simultaneously subtracting the  $g$ -mode frequencies  $f_3$ ,  $f_4$  and  $f_5$  results in the residual LSP (bottom). Horizontal lines indicate confidence levels of  $3\sigma$ ,  $2\sigma$  and  $1.5\sigma$ .

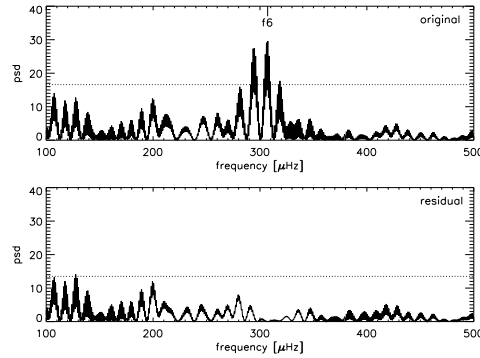


Figure 4. LSPs of the  $g$ -mode regime of HS 2201+2610 after subtraction of five  $p$ -modes (top). Subtracting the  $g$ -mode frequency  $f_6$  results in the residual LSP (bottom). Horizontal lines indicate  $3\sigma$  confidence levels.

**Acknowledgments.** R. Lutz thanks the organizers for providing financial support. Based on observations at the CAHA at Calar Alto, operated by MPIA and CSIC. DFG travel grants DR 281/20-1 and SCHU 2249/3-1.

## References

- Charpinet, S., Fontaine, G., Brassard, P., et al. 1997, *ApJ*, 483, L123  
 Dorman, B., O’Connell, R. W., & Rood, R. T. 1995, *ApJ*, 442, 105  
 Fligge, M. & Solanki, S. K. 1997, *A&AS*, 124, 579  
 Fontaine, G., Brassard, P., Charpinet, S., et al. 2003, *ApJ*, 597, 518  
 Green, E. M., Fontaine, G., Reed, M. D., et al. 2003, *ApJ*, 583, L31  
 Jeffery, C. S. & Saio, H. 2006, *MNRAS*, 372, L48  
 Kilkeny, D., Koen, C., O’Donoghue, D., & Stobie, R. S. 1997, *MNRAS*, 285, 640  
 Schuh, S., Dreizler, S., Deetjen, J. L., & Göhler, E. 2003, *BaltA*, 12, 167  
 Schuh, S., Huber, J., Dreizler, S., et al. 2006, *A&A*, 445, L31  
 Silvotti, R., Janulis, R., Schuh, S., et al. 2002, *A&A*, 389, 180  
 Silvotti, R., Schuh, S., Janulis, R., et al. 2007, *Nature*, 449, 189